Arch Biol Sci. 2023;75(2):237-245 https://doi.org/10.2298/ABS230313019S

Elevated barometric pressure suppresses cell proliferation by delaying the G2/M phase and weakening integrin-mediated cell adhesion and actin assembly

Gwang-ic Son[1,2], Eunil Lee[1,2,*], Mari Kim[1,2], Seoeun Lee[1,2], Yesol Moon[1,2] and Joonhee Kim[1,2]

[1]*Department of Preventive Medicine, College of Medicine, Korea University*, 73 Goryeodae-ro, Seongbuk-gu, Seoul 02841, Republic of Korea

[2]*Department of Medical Science Graduate School, Korea University*, 73 Goryeodae-ro, Seongbuk-gu, Seoul 02841, Republic of Korea

***Corresponding author**: eunil@korea.ac.kr

Received: March 13, 2023; **Revised**: April 17, 2023; **Accepted**: April 18, 2023; **Published online**: May 16, 2023

Abstract: Human cells are continuously exposed to various stress factors in their physiological environment. Evidence suggests that certain mechanical stress can affect cell cycle progression and cell proliferation. However, the signaling pathways involved in this process are not well understood. To investigate this, we developed a pressure chamber capable of producing an elevated barometric pressure (EBP) environment of 2×atmospheric absolute pressure (ATA). We then studied the effect of EBP on cell proliferation and its underlying mechanism. Our results show that EBP inhibited cell proliferation by delaying the G2/M phase. Specifically, EBP reduced the expression levels of cell adhesion-related genes and downregulated integrin subunit genes, resulting in weaker interaction between cells and extracellular matrix proteins. In addition, Ras-related C3 botulinum toxin substrate 1 (Rac1) and cell division control protein 42 homolog (Cdc42) activity was suppressed, and actin assembly was decreased. These findings suggest that the EBP-mediated G2/M phase delay is due to attenuated cell adhesion and actin cytoskeleton assembly, leading to the inhibition of cell proliferation. Our results provide a crucial molecular mechanism for how certain pressure (changes) can negatively regulate cell proliferation. These findings could potentially be used in the future to develop a pressure therapy to inhibit cell proliferation in cancer patients.

Keywords: elevated barometric pressure, cell proliferation, cell cycle, cell adhesion, actins

INTRODUCTION

Hyperbaric oxygen therapy (HBO) is used to treat hypoxia and chronic wounds by intermittently applying oxygen concentrations of 95% or greater than that of ambient air. The preferred pressure range for the therapy is 2-2.5 ATA [1]. Moreover, there have been many cancer therapy studies using HBO showing that 2.5 ATA significantly reduced tumor size in mice injected with A549 cells (lung cancer cell line) [2], and that 2.5-ATA decreased cancer-associated fibroblasts and enhanced the antitumor efficacy of combined paclitaxel and gemcitabine therapy [3]. These results provide an important indication that a certain mechanical pressure may play a role in cancer control.

Compressive stress is a type of pressure that compresses an object and is often observed in cellular physiological environments. Compressive stress even affects ion channel activities, which, in turn, leads to the triggering of subsequent intracellular signal pathways [4]. In effect, it regulates rho-associated, coiled-coil-containing protein kinase 1/Ras homolog family member A (RhoA) family of GTPases (ROCK/Rho-GTP) and phosphoinositide 3-kinase (PI3K) pathways via actin depolymerization caused by Ca2+ signaling [5,6].

As for tumorigenesis, pressure loading can control the size of tumor spheroids by suppressing proliferation and inducing apoptosis in cancer cells [7]. Notably, our previous studies revealed that compressive stress up to 2 ATA inhibited cell proliferation in H460 and WI38 cells [8,9]. Although pressure stress negatively modulates cell proliferation in organisms, the corresponding mechanism is not yet fully understood. Therefore, in the present study, we developed an in-

house pressure device that can generate pure hyperbaric conditions without oxygen toxicity by mimicking the HBO environment and defined this environment as elevated barometric pressure (EBP). We investigated the molecular mechanism of EBP-mediated cell proliferation inhibition in H460 non-small cell lung carcinoma. Our results showed that EBP inhibited cell proliferation mainly by prolonging the G2/M phase. This phenomenon seems to be due to cell adhesion disruption and weakened actin assembly along with decreased Rac1 and Cdc42 activity. Our results provide fundamental insights into how EBP regulates the cell cycle and suggest that EBP-mediated inhibition of cell proliferation may benefit cancer patients by delaying cancer progression.

MATERIALS AND METHODS

Cell lines and culture

H460, A549, H1299 and WI-38 cells were sourced from the American Type Culture Collection (ATCC) (Manassas, VA, USA). The non-small cell lung carcinoma (NSCLC) cell lines A549, H460 and H1299 were cultured in RPMI 1640 medium containing 10% fetal bovine serum (Gibco BRL, Grand Island, USA) and antibiotics (Gibco BRL) in an incubator set at 37°C and 5% CO2 atmosphere. WI-38 cells, a normal fetal lung fibroblast line, were maintained in Dulbecco's modified Eagle's medium (DMEM; Gibco BRL). The cell culture under EBP to 2 ATA, using a customized chamber, was conducted as described previously [10]. The EBP is twice the atmospheric pressure, but the amount of oxygen remains the same as at normal atmospheric pressure, thus avoiding oxygen toxicity.

Cell counting assay and cell survival assay

A549 (1.0(105 cell/mL), H460 (1.0(105 cell/mL), H1299 (1.0(105 cell/mL) and WI-38 (1.0(105 cell/mL) cells were seeded into a 60-mm dish and subjected to EBP and control conditions for 48 h. Cells were counted using the AccuChip Kit (NanoEntek, Korea) and ADAM-MC automatic cell counter (Digital Bio, Germany) according to the manufacturers' instructions. Cells were trypsinized and AccuStain Solution T in the AccuChip Kit was used for total cell counting. Only non-viable cells were stained and detected by AccuStain Solution N in the AccuChip Kit. The prepared cells were loaded into the chip in the AccuChip Kit. Viability was automatically calculated in the software ADAM-MC (NanoEntek, Korea) after each measurement of total cells and nonviable cells. The assays were performed in triplicate.

Cell cycle analysis

H460 cells were treated with trypsin (Gibco BRL) and pellets were harvested by centrifugation at 1000×*g* for 90 s after washing with phosphate-buffered saline (PBS). The harvested cells were fixed with 70% ethanol at 4°C overnight. Fixed cells were washed to remove ethanol, resuspended in 1 mL PBS containing RNase (100 μg/mL) and propidium iodide (PI, 10 μg/mL) and incubated for 20 min at room temperature in the dark. Analyses were performed by fluorescence-activated cell sorting (FACS). The PI excitation and emission wavelengths were 488 nm and 640 nm, respectively. Data were analyzed using WinMDI (multiple document interfaces for Windows).

Sequencing

mRNA-sequencing analysis was conducted in H460 cells exposed to EP for 36 h. Transcription libraries were prepared for sequencing on the Illumina GAIIX platform using the RNA-seq kit (Part no. 1004898 Rev. A) according to the manufacturer's protocol. Briefly, purified RNA was fragmented by 5 min of incubation with Illumina-supplied fragmentation buffer at 94°C. The first cDNA strand was then synthesized by reverse transcription using random oligo primers. Second-strand synthesis was conducted by incubation with RNase H and DNA polymerase I. The resulting double-stranded DNA fragments were end-repaired, and A-nucleotide overhangs were added by incubation with Taq Klenow fragment lacking exonuclease activity. After the attachment of anchor sequences, fragments were PCR-amplified using Illumina-supplied primers and loaded onto the GAIIX flow cell. Image analysis and base calling were conducted with Firecrest and Bustard programs, respectively, and initial sequence alignment for QC purposes was performed using Eland.

GTPase activity assay

The amounts of active GTP-bound Rac1, Cdc42 and RhoA were determined using Rac1, Cdc42 and RhoA G-LISA activation assay kits (Cytoskeleton Inc., Denver, CO, USA) according to the manufacturer's instructions. H460 cells were exposed to EBP for 48 h and harvested at 12-h intervals. Protein lysates were collected for subsequent analysis using G-LISA; constitutively active RhoA, Cdc42 and Rac1 proteins were used as positive controls. Absorbance was measured using a microplate reader at 490 nm to obtain the relative activities.

G/F-actin ratio *in vivo* assay

The G/F-actin ratio *in vivo* assay was conducted in H460 cells. Proteins were extracted and analyzed using the F-actin/G-actin *in vivo* assay kit (Cytoskeleton Inc., Denver, CO, USA) according to the manufacturer's instructions. Briefly, cells were lysed in a detergent-based buffer that dissolved G-actin but not F-actin. F-actin was pelleted by centrifugation while leaving G-actin in the supernatant. Actin in the pellet and supernatant was quantitated by Western blotting. The grayscale value of each band was measured using ImageJ software.

Cell adhesion assay

Cell adhesion assays were performed using CytoSelect 48-well cell adhesion assay kits (Cell Biolabs Inc., San Diego, CA; catalog no. CBA-070) to confirm the degree of extracellular matrix components such as fibronectin, collagen I, collagen IV, laminin I and fibrinogen. A total of 1.0×10^6 H460 cells/mL in 150 µL of serum-free medium were added to each well and incubated for 1 h at 37°C. After careful removal of the medium, the wells were washed four times with 150 µL PBS to evaluate the attached cells. Cell staining was performed with a Cell staining solution kit. Absorbance was measured using a microplate reader at 560 nm to obtain the relative activities.

Statistical analysis

Statistical significance between EBP and matching controls was analyzed using GraphPad Prism software version 9.0 (GraphPad, San Diego, USA). Data between EBP and control were analyzed with an unpaired t-test. Statistical significance was set at $P<0.05$, and data are presented as mean±standard error of the mean.

RESULTS

EBP inhibits cell proliferation without cell death

To observe the effect of EBP on cell proliferation, H460 cells were counted at 4-h intervals over a 48-h culture period. After 24 h of EBP incubation, the number of cells in the control (2.89×10^5 cell/mL) began to increase more rapidly than that in the EBP sample (2.39×10^5 cell/mL). Importantly, after 36 h post-incubation, there were significant differences in the cell count between the two groups (Fig. 1A). In addition, we examined the trend of doubling time in H460 using the cell count results. The number of cells in both control ($y=0.8853e^{0.1666x}$; $R^2=0.989$) and EBP ($y=0.9134e^{0.1462x}$; $R^2=0.979$) increased exponentially over time. As a result of estimating the doubling time of control and EBP using their respective exponential formulas, the doubling time of control and EBP was about 16.3 and 18.4 h, respectively. These results not only mean that the doubling time of EBP was delayed by 2.1 h compared to the control, but also suggest that the cell cycle delay occurs with every doubling time.

To assess the cell toxicity of EBP, we measured the cell survival rate by counting the number of living and dead cells every 4 h. All measured cell viabilities were above 80%, with no statistical differences between the EBP and control groups (Fig. 1B). Other cell lines such as A549, H1299 and WI38 also showed statistically significant differences in cell numbers between the two groups at 48 h post-incubation (Fig. 1C). These results demonstrate that EBP negatively affected cell proliferation and is not cytotoxic.

EBP delays cell cycle progression in the G2/M phase

To determine the point at which the cell cycle was delayed, we observed the cell cycle for 32 h, twice the time of cell proliferation. FACS was used to determine the cell distribution in H460 cells in each cell cycle phase, including the G0/G1, S and G2/M phases, every 4 h after synchronizing the cells at late G0/G1 phase.

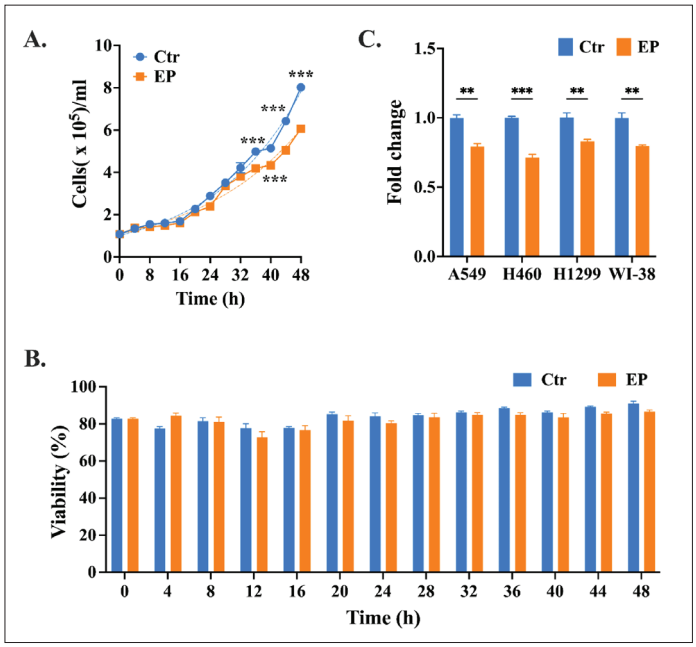

Fig. 1. Post- EP incubation, cell proliferation is significantly suppressed in multiple cell lines with no cell death. **A** – H460 cells were exposed to EP for 48 h, and cell counting assays were conducted every 4 h using the ADAM Cell Counter. The doubling time of the control and EBP was determined by calculating the time required for their quantities to increase 2-, 4- and 8-fold using their respective exponential formulas. **B** – Cell viability was assessed in H460 cells at EP for 48 h. Cell survival rates were calculated by comparing the numbers of living and dead cells against the total number of cells. **C** – At 48 h post-EP incubation, cell counting analysis was performed in H460, A549, H1299 and WI-38 cell lines. Asterisks indicates statistically significant differences compared to the control group *(P<0.05), **(P<0.01) and ***(P<0.001).

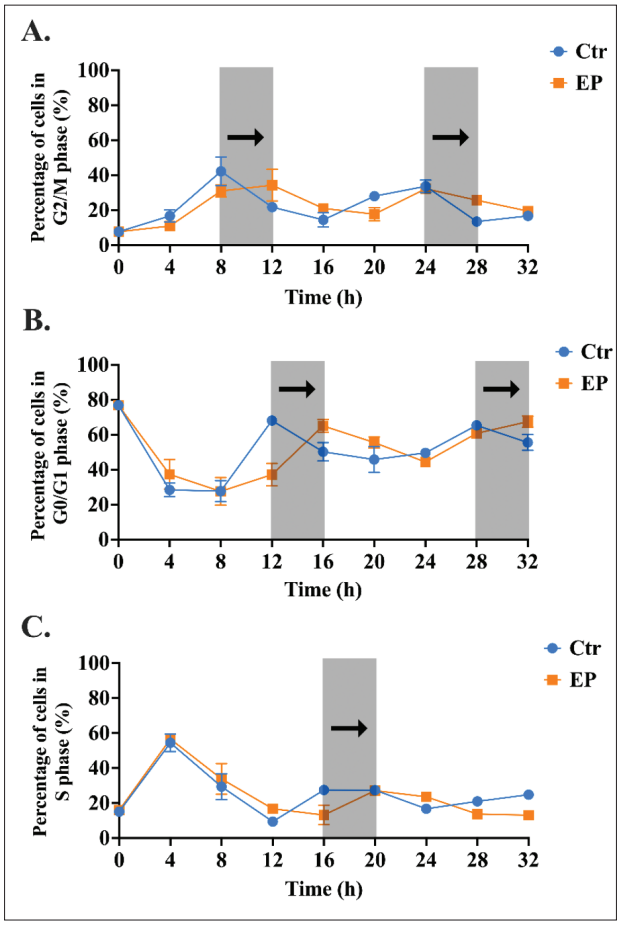

Fig. 2. Cell cycle progression was delayed in the G2/M phase under EP. G0/G1 phase synchronization was performed by culturing H460 cells in serum-starved media for 24 h. After synchronization, the cells were exposed to EP for 32 h. During EBP exposure, cell distribution in the G2/M phase (**A**), G0/G1 phase (**B**), and S phase (**C**) were measured every 4 h using FACS analysis.

After synchronization, about 80% of the cells were in the G0/G1 phase in both control and EBP. The first cell cycle delay was observed in the G2/M phase. The peak percentage of cells in this phase was reached at 8 h of incubation in the control and at 12 h in the EBP (Fig. 2A). This delay carried over into the next phase, showing that the peak percentage of cells in the G0/G1 phase was in the control at 12 h, but at 16 h in the EBP (Fig 2B). In the S phase, the first peaks were found at 4 h in both EBP and control groups. However, for G0/G1, the second peak in the control (16 h) occurred 4 h earlier than that in the EBP group (20 h) (Fig. 2C). We observed the same delay in subsequent cell cycles, which occurred 16 h after the peak percentage was exceeded. In summary, delayed G2/M phase cell cycle progression in EBP was maintained in the G0/G1 and S phases. These results show that the delay in cell cycle progression occurs specifically in the G2/M phase and not throughout the cycle, which is key evidence for EBP-mediated inhibition of cell proliferation. Furthermore, based on the results of cell proliferation (Fig. 1A), we suggest that the G2/M phase continued to be delayed after 32 h.

EBP changes the expression levels of cell adhesion-related genes

To identify the biological alteration that caused the EBP-mediated inhibition of cell proliferation, we performed mRNA sequencing analysis in H460 cells at 36 h post-incubation. We selected genes exhibiting more than a 1.5-fold change in expression based on over five read counts. Of the 4,853 altered genes, 1,794 had increased

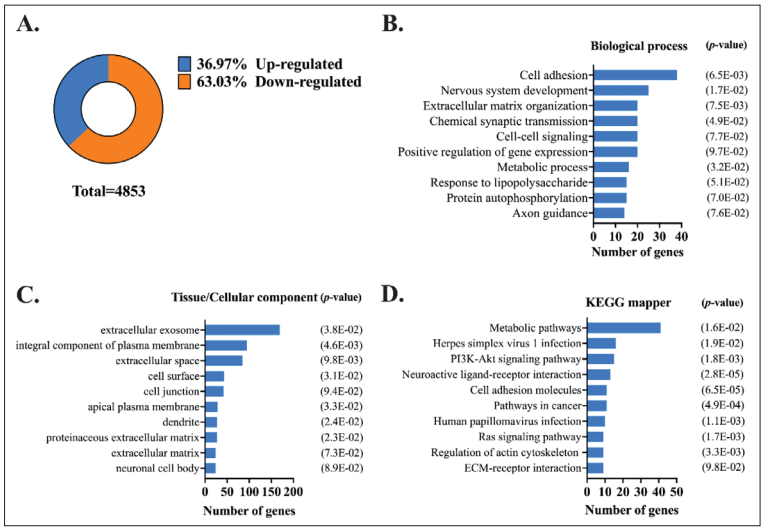

Fig. 3. The mRNA expression levels of cell adhesion-related genes were markedly reduced under EP. **A** – mRNA-sequencing analysis conducted in H460 cells at 36 h post-exposure to EP, showing respectively the percentages of genes with their expression upregulated and downregulated. Analysis of biological processes (**B**) and tissue/cellular components (**C**) on the Quick-Go website showed the number of genes in each category. **D** – Mechanistic pathway analysis by the KEGG Mapper showed the genes with altered expression levels in major pathways in response to EP.

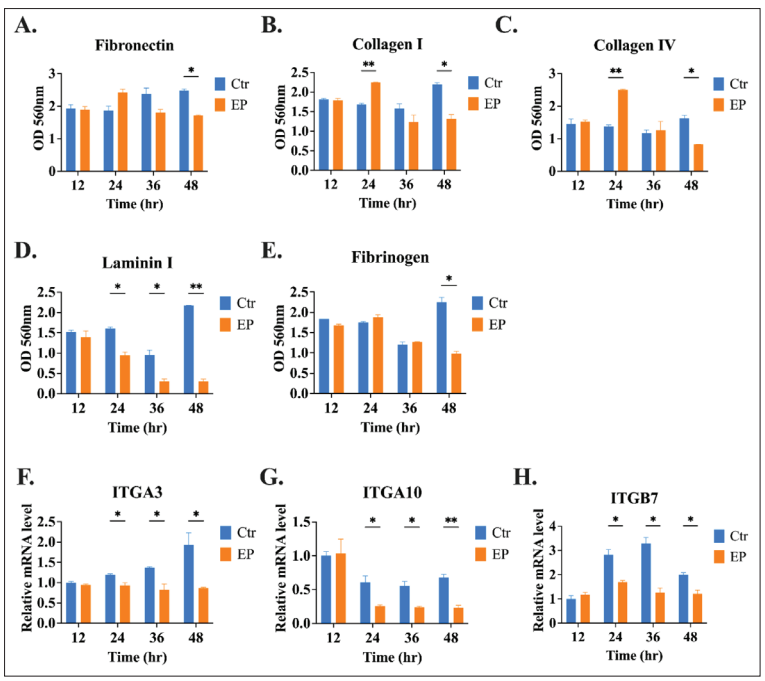

Fig. 4. In the EP condition, the number of cells interacting with ECM proteins significantly decreases and integrins are significantly downregulated. H460 cells were exposed to EP for 48 h and cell adhesion to fibronectin (**A**), collagen I (**B**), collagen IV (**C**), laminin (**D**) and fibrinogen (E) was measured every 12 h for 48 h using a cell adhesion assay. The relative mRNA levels of ITGA3 (**F**), ITGA10 (**G**), and ITGB7 (**H**) were determined using a qRT-PCR technique. Three biological replicates per experimental condition were used for the calculation. Asterisks indicate statistically significant differences in comparison to the control group *(P<0.05), **(P<0.01) and ***(P<0.001).

expression, while 3,059 had decreased expression (Fig. 3A). These changed genes were classified into two main categories through gene ontology (GO) using DAVID and analyzing the biological process (BP) and tissue/cellular components (CC). Among these categories, cell adhesion altered the most in the BP categories. The changed BP category also included extracellular matrix organization and cell-cell signaling as top subcategories (Fig. 3B). Similarly, CC categories identified significant changes in genes localized in cell membranes and outside cells, such as extracellular exosome, extracellular space, cell surface, cell junction and extracellular matrix (Fig. 3C). Next, we performed the KEGG mapping using the mRNA sequencing data to identify signaling pathways related to the EBP-mediated cell cycle delay. Interestingly, the subcategories of the KEGG mapper included cell adhesion molecules (CAMs), consistent with the BP result showing altered cell adhesion. Additionally, the signaling pathway related to the regulation of the actin cytoskeleton, which is directly related to cell adhesion, also showed significant changes (Fig. 3D). Collectively, these results suggested that the EBP-mediated inhibition of cell proliferation was mainly associated with cell-ECM adhesion modifications.

EBP attenuates cell adhesion by suppressing integrin expression

To verify the results obtained from the mRNA sequencing, we performed a cell adhesion assay at 12-h intervals to explore the changes in the cell adhesion phenotypes for each extracellular matrix (ECM) protein in H460. The number of H460 cells attached to fibronectin (Fig. 4A), collagen I (Fig. 4B), collagen IV (Fig. 4C), laminin I (Fig. 4D) and fibrinogen (Fig. 4E), respectively, were all diminished significantly at 48 h post-EBP incubation. As for cell adhesion to laminin I, the

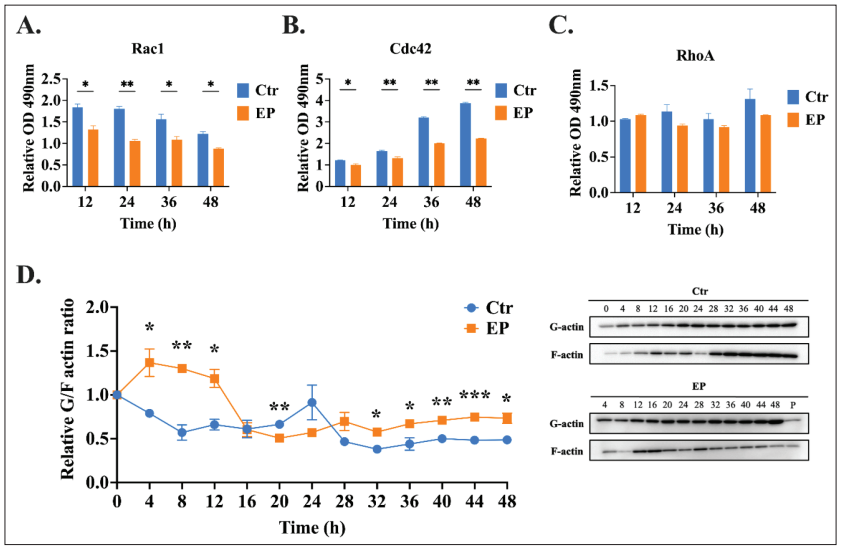

Fig 5. EP inhibits Rac1 and Cdc42 GTPase activity, but not RhoA, and EP increases the G/F actin ratio. H460 cells were exposed to EP for 48 h and Rac1 (**A**), Cdc42 (**B**) and RhoA (**C**) activity was measured every 12 h using an ELISA-based activity assay. **D** – The G- and F-actin levels of the cells were measured every 4 h until 48 h in the EP and normal conditions, respectively, using Western blotting, then the G/F actin ratio was calculated. Asterisks indicate statistically significant differences in comparison to the control group *(P<0.05), **(P<0.01), and ***(P<0.001).

number of affected cells decreased significantly from 24 h onwards (Fig. 4D).

The integrins combine with the ECM to transmit extracellular signals into the cell and are directly involved in cell adhesion [11]. Therefore, we confirmed the mRNA expression levels of genes encoding integrin subunits such as integrin subunit alpha 3 (ITGA3), integrin subunit alpha 10 (ITGA10) and integrin subunit beta 7 (ITGB7), which were found to have decreased under the EBP in the earlier mRNA-sequencing data. Interestingly, the mRNA expression levels of ITGA3, ITGB7 and ITGA10 genes significantly decreased in EBP compared to the control from 24 h post-incubation (Fig. 4 F, G, and H). Collectively, these results showed that EBP significantly weakened cell adhesion by downregulating integrin subunit genes.

EBP inhibits Rac1 and Cdc42 activity and decreases actin assembly

The mRNA sequencing results showed changes in genes associated with the regulation of the actin cytoskeleton. According to previous studies, the assembly of the actin cytoskeleton is regulated by Rho GTPases, such as Rac1, Cdc42 and RhoA [12]. In addition, a decrease in actin assembly can reduce cell adhesion [13]. We assumed that the reduced cell adhesion was due to decreased actin assembly. To verify this, we measured the activity of Rho GTPase and the G/F actin ratio. First, we measured the activity of Rho GTPases including RhoA, Rac1 and Cdc42 every 12 h for 48 h. Rac1 and Cdc42 activities were significantly suppressed in the EBP compared to the control group at all time points (Fig. 5A, B). However, there was no significant difference in the activity of RhoA between the two groups (Fig. 5C). Next, the G/F actin ratio was measured to investigate the level of actin polymerization in H460 cells. The G/F actin ratio increased overall in the EBP group and showed a significant decrease between the EBP and control groups at all post-incubation time points, except at 16, 20, 24 and 28 h (Fig. 5D). Collectively, these results suggest that EBP interrupted integrin-mediated cell adhesion by lowering Rac1 and Cdc42 activity and weakening actin polymerization.

DISCUSSION

The present study demonstrates that EBP is a critical factor that can regulate cell proliferation and provides information on the probable molecular mechanism. Our results show that EBP suppresses cell proliferation by delaying the G2/M phase, which is closely related to weakened integrin-mediated cell adhesion and actin assembly.

The effect of pressure on cell proliferation can depend on various factors, such as the type of cells being studied and the strength or magnitude of the pressure. Previous studies have shown that the proliferation of vascular smooth muscle cells increases with elevations of static pressure (60 and 90 mmHg), and peaks at pressures 120 mm Hg above atmospheric pressure; however, it decreases at higher pressures of 150- and 180-mm Hg [14]. These previous research results suggest that high pressure has a negative impact on cell proliferation, with which our results agree. In

addition, cell proliferation due to pressure has shown various results depending on the cell line. Generally, there are many reports that indicate a decrease in cell proliferation in cancer cell lines [15-18], while there are many reports that indicate an increase in cell proliferation in normal cell lines [19,20]. These results suggest that the effect of pressure on cell proliferation may differ depending on the characteristics of the cancer cells and the normal cells. However, while there are reports that HBO increases cell proliferation in normal cell lines, EBP has been shown to inhibit cell proliferation in WI-38, which is consistent with our previous research report [9]. Previous studies have suggested that an increase in oxygen pressure may be responsible for the observed increase in cell proliferation under HBO [19,20]. High oxygen partial pressure may increase oxygen delivery to cells, enhancing cellular metabolism and energy production [21]. EBP has a lower oxygen partial pressure compared to HBO because it contains the same amount of oxygen as in the atmosphere. Therefore, the difference in cell proliferation under high pressure may be due to differences in cellular metabolism caused by variations in oxygen partial pressure.

We observed that ECM-cell adhesion, including ITGA3, ITGA10 and ITGB7 mRNA levels, were significantly decreased under EBP. In agreement with previous studies, we show that the levels of ITGA3 and ITGA10 decreased when human tenocytes were exposed to mechanical stress, which may be a cause of decreased cell adhesion [22]. Thus, it can be interpreted that EBP reduced cell-ECM adhesion in H460 cells by downregulating ITGA3, ITGA10 and ITGB7 genes; in addition, integrins regulate the activity of Rac1 and Cdc42. [23]. This suggests that the reduction in Rac1 and Cdc42 activity under EBP is due to the downregulation of the ITGA3, ITGA10, and ITGB7 genes. Moreover, the reduction in Rac1 and Cdc42 activity by integrins can weaken the assembly of the actin cytoskeleton [12]. Indeed, our study demonstrated that the assembly of F-actin was alleviated along with the reduction in Rac1 and Cdc42 activity under EBP. This suggests that the reduction in Rac1 and Cdc42 activity is indicative of weakened cell-ECM adhesion and is also the cause of weakened actin assembly.

In effect, actin assembly is deeply engaged in cell proliferation and cycle progression. According to previous studies, mitotic progression can be delayed by actin depolymerization induced by cytochalasin D or latrunculin B [24, 25], but was promoted by actin polymerization induced by protein mutation or jasplakinolide in Wiskott-Aldrich syndrome [26]. Of note, weakened actin assembly can also delay cell cycle progression [27], and actin dysfunction delays G2/M phase [28]. These results suggest that cell cycle progression depends on the degree of actin cytoskeleton assembly and can be delayed when the assembly is weakened, such as under altered pressure conditions. However, there is insufficient evidence to determine the cause of how the reduction in cell adhesion and actin assembly specifically contributes to the delay in G2/M phase. According to one study, actin assembly is required for the transition from G2/M to G1 since cells are unstable without cell adhesion because of deficient actin assembly [29]. This could be the explanation why the G2/M phase was delayed under EBP and that this event was related to weakened cell adhesion and insufficient actin assembly.

We note that consistent with this interpretation, previous studies have also provided important evidence that integrin-mediated cell adhesion influences cell progression. Specifically, weakened cell adhesion delayed the M phase in cancer cells [30], and in prostate cancer cells anticancer therapy relieved tumor cell adhesion and delayed the cell cycle suppressing cancer progression [31]. These results suggest that a weakened interaction between cells and ECM proteins underlies the cell cycle delay. A crucial link between the EBP-mediated delay of G2/M phase detected in our study can be attributed to the reduced expression of integrin subunits and the consequent weakening of cell ECM adhesion and actin assembly.

Taken together, this study provides important evidence that EBP can suppress cell proliferation by delaying the G2/M phase in cancer cells. This is intimately connected with weakened cell adhesion and actin cytoskeleton assembly. If further research is conducted to verify the anticancer effect of EBP in mammals and to determine the appropriate exposure duration and interval for clinical use, it is expected that cancer treatment based on EBP can be used in clinical therapy.

Funding: This work was supported by the Korea Environment Industry and the Technology Institute (KEITI) through the Environmental Health Action Program funded by the Korea Ministry of Environment (MOE) (2017001360006).

Author contributions: Study conception and design: Eunil Lee, Gwang-ic Son and Joonhee Kim; acquisition of data: Gwang-ic Son, Seoeun Lee and Yesol Moon; analysis and interpretation data: Gwang-ic Son, Eunil Lee, Mari Kim, Seoeun Lee, Yesol Moon and Joonhee Kim; manuscript writing and editing: Gwang-ic Son and Eunil Lee.

Conflict of interest disclosure: All authors declare that there are no competing interests or personal relationships that could have influenced the work reported in this paper.

Data availability: Data underlying the reported findings have been provided as part of the submitted article and are available at: https://www.serbiosoc.org.rs/NewUploads/Uploads/Son%20et%20al_8512-Data%20Set.xlsx

REFERENCES

1. Benedetti S, Lamorgese A, Piersantelli M, Pagliarani S, Benvenuti F, Canestrari F. Oxidative stress and antioxidant status in patients undergoing prolonged exposure to hyperbaric oxygen. Clin Biochem. 2004;37(4):312-7. https://doi.org/10.1016/j.clinbiochem.2003.12.001
2. Chen S-Y, Tsuneyama K, Yen M-H, Lee J-T, Chen J-L, Huang S-M. Hyperbaric oxygen suppressed tumor progression through the improvement of tumor hypoxia and induction of tumor apoptosis in A549-cell-transferred lung cancer. Sci Rep. 2021;12(9):e0185394. https://doi.org/10.1038/s41598-021-91454-2
3. Wanga X, Ningbing Yea, Chen Xua, Chen Xiaoa, Zhijie Zhanga, Qingyuan Denga, Lia S, Lia J, Li Z, Yang X. Hyperbaric oxygen regulates tumor mechanics and augments Abraxane and gemcitabine antitumor effects against pancreatic ductal adenocarcinoma by inhibiting cancer-associated fibroblasts. Nano Today. 2022;44:101458. https://doi.org/10.1016/j.nantod.2022.101458
4. Cox CD, Bavi N, Martinac B. Origin of the Force: The Force-From-Lipids Principle Applied to Piezo Channels. Curr Top Membr. 2017;79:59-96. https://doi.org/10.1016/bs.ctm.2016.09.001
5. Kim J, Montagne K, Nemoto H, Ushida T, Furukawa KS. Hypergravity down-regulates c-fos gene expression via ROCK/Rho-GTP and the PI3K signaling pathway in murine ATDC5 chondroprogenitor cells. PLoS One. 2017;12(9):e0185394. https://doi.org/10.1371/journal.pone.0185394
6. Mishra R, van Drogen F, Dechant R, Oh S, Jeon NL, Lee SS, Peter M. Protein kinase C and calcineurin cooperatively mediate cell survival under compressive mechanical stress. Proc Natl Acad Sci U S A. 2017;114(51):13471-6. https://doi.org/10.1073/pnas.1709079114
7. Cheng G, Tse J, Jain RK, Munn LL. Micro-environmental mechanical stress controls tumor spheroid size and morphology by suppressing proliferation and inducing apoptosis in cancer cells. PLoS One. 2009;4(2):e4632. https://doi.org/10.1371/journal.pone.0004632
8. Oh S, Kwon D, Lee HJ, Kim J, Lee E. Role of elevated pressure in TRAIL-induced apoptosis in human lung carcinoma cells. Apoptosis. 2010;15(12):1517-28. https://doi.org/10.1007/s10495-010-0525-5
9. Oh S, Lee E, Lee J, Lim Y, Kim J, Woo S. Comparison of the effects of 40% oxygen and two atmospheric absolute air pressure conditions on stress-induced premature senescence of normal human diploid fibroblasts. Cell Stress Chaperones. 2008;13(4):447-58. https://doi.org/10.1007/s12192-008-0041-5
10. Oh S, Kim Y, Kim J, Kwon D, Lee E. Elevated pressure, a novel cancer therapeutic tool for sensitizing cisplatin-mediated apoptosis in A549. Biochem Biophys Res Commun. 2010;399(1):91-7. https://doi.org/10.1016/j.bbrc.2010.07.047
11. Arnaout MA, Goodman SL, Xiong JP. Structure and mechanics of integrin-based cell adhesion. Curr Opin Cell Biol. 2007;19(5):495-507. https://doi.org/10.1016/j.ceb.2007.08.002
12. Spiering D, Hodgson L. Dynamics of the Rho-family small GTPases in actin regulation and motility. Cell Adh Migr. 2011;5(2):170-80. https://doi.org/10.4161/cam.5.2.14403
13. Michael M, Yap AS. The regulation and functional impact of actin assembly at cadherin cell-cell adhesions. Semin Cell Dev Biol. 2013;24(4):298-307. https://doi.org/10.1016/j.semcdb.2012.12.004
14. Luo DX, Cheng J, Xiong Y, Li J, Xia C, Xu C, Wang C, Zhu B, Hu Z, Liao D. Static pressure drives proliferation of vascular smooth muscle cells via caveolin-1/ERK1/2 pathway. Biochem Biophys Res Commun. 2010;391(4):1693-7. https://doi.org/10.1016/j.bbrc.2009.12.132
15. Granowitz EV, Tonomura N, Benson RM, Katz DM, Band V, Makari-Judson GP, Osborne BA. Hyperbaric oxygen inhibits benign and malignant human mammary epithelial cell proliferation. Anticancer Res. 2005;25(6B):3833-42.
16. McIntyre KM, Dixon PS, Krock LP, Piepmeier EH, Jr. The influence of hyperbaric oxygenation on leukocyte viability and surface protein expression. Aviat Space Environ Med. 1997;68(12):1129-33.
17. Petre PM, Baciewicz FA, Tigan S, Spears JR. Hyperbaric oxygen as a chemotherapy adjuvant in the treatment of metastatic lung tumors in a rat model. J Thorac Cardiov Sur. 2003;125(1):85-95. https://doi.org/10.1067/mtc.2003.90
18. Chen YC, Chen SY, Ho PS, Lin CH, Cheng YY, Wang JK, Sytwu HK. Apoptosis of T-leukemia and B-myeloma cancer cells induced by hyperbaric oxygen increased phosphorylation of p38 MAPK. Leuk Res. 2007;31(6):805-15. https://doi.org/10.1016/j.leukres.2006.09.016
19. Tompach PC, Lew D, Stoll JL. Cell response to hyperbaric oxygen treatment. Int J Oral Maxillofac Surg. 1997;26(2):82-6. https://doi.org/10.1016/S0901-5027(05)80632-0
20. Piepmeier EH, Kalns JE. Fibroblast response to rapid decompression and hyperbaric oxygenation. Aviat Space Environ Med. 1999;70(6):589-93.
21. Wilson DF. Oxidative phosphorylation: regulation and role in cellular and tissue metabolism. J Physiol. 2017;595(23):7023-38. https://doi.org/10.1113/JP273839

22. Jones ER, Jones GC, Legerlotz K, Riley GP. Mechanical regulation of integrins in human tenocytes. Int J Exp Pathol. 2013;94(4):A17-A.
23. Keely PJ, Westwick JK, Whitehead IP, Der CJ, Parise LV. Cdc42 and Rac1 induce integrin-mediated cell motility and invasiveness through PI(3)K. Nature. 1997;390(6660):632-6. https://doi.org/10.1038/37656
24. Gachet Y, Tournier S, Millar JB, Hyams JS. A MAP kinase-dependent actin checkpoint ensures proper spindle orientation in fission yeast. Nature. 2001;412(6844):352-5. https://doi.org/10.1038/35085604
25. Lee K, Song K. Actin dysfunction activates ERK1/2 and delays entry into mitosis in mammalian cells. Cell Cycle. 2007;6(12):1487-95. https://doi.org/10.4161/cc.6.12.4303
26. Moulding DA, Blundell MP, Spiller DG, White MR, Cory GO, Calle Y, Kempski H, Sinclair J, Ancliff PJ, Kinnon C, Jones GE, Thrasher AJ. Unregulated actin polymerization by WASp causes defects of mitosis and cytokinesis in X-linked neutropenia. J Exp Med. 2007;204(9):2213-24. https://doi.org/10.1084/jem.20062324
27. Hussey PJ, Ketelaar T, Deeks MJ. Control of the actin cytoskeleton in plant cell growth. Annu Rev Plant Biol. 2006;57:109-25. https://doi.org/10.1146/annurev.arplant.57.032905.105206
28. Shrestha D, Choi D, Song K. Actin Dysfunction Induces Cell Cycle Delay at G2/M with Sustained ERK and RSK Activation in IMR-90 Normal Human Fibroblasts. Mol Cells. 2018;41(5):436-43.
29. Lamarche N, Tapon N, Stowers L, Burbelo PD, Aspenstrom P, Bridges T, Chant J, Hall A. Rac and Cdc42 induce actin polymerization and G1 cell cycle progression independently of p65PAK and the JNK/SAPK MAP kinase cascade. Cell. 1996;87(3):519-29. https://doi.org/10.1016/S0092-8674(00)81371-9
30. Ungai-Salanki R, Haty E, Gerecsei T, Francz B, Beres B, Sztilkovics M, Szekacs I, Szabo B, Horvath R. Single-cell adhesion strength and contact density drops in the M phase of cancer cells. Sci Rep. 2021;11(1):18500. https://doi.org/10.1038/s41598-021-97734-1
31. Wedel S, Hudak L, Seibel JM, Makarevic J, Juengel E, Tsaur I, Waaga-Gasser A, Haferkamp A, Blaheta RA. Molecular targeting of prostate cancer cells by a triple drug combination down-regulates integrin driven adhesion processes, delays cell cycle progression and interferes with the cdk-cyclin axis. BMC Cancer. 2011;11:375. https://doi.org/10.1186/1471-2407-11-375